C.D.I. TECH NOTE 82-31

# MARK I VACUUM BREAKER IMPROVED VALVE DYNAMIC MODEL - MODEL DEVELOPMENT AND VALIDATION

Revision 0

Prepared by

John M. Sullivan
CONTINUUM DYNAMICS, INC.
P.O. BOX 3073
PRINCETON, NEW JERSEY 08540

Prepared Under Purchase Order No. 205-XJ102 For

THE GENERAL ELECTRIC COMPANY
175 CURTNER AVENUE
SAN JOSE, CALIFORNIA 95125

Approved by

Alan Bilanin

Alan J. Bilanin



August, 1982

## DISCLAIMER OF RESPONSIBILITY

CONTENTS

## ILLUSTRATIONS

## TABLES

## SUMMARY

Earlier studies of Mark I vacuum breaker dynamics to determine valve impact velocities used an overly conservative analytic valve model. Comparison of its predictions with measured valve position from FSTF run S-DA showed that valve velocities were overpredicted by 150%. This report describes the development of a new valve dynamic model which computes the spatial harmonics of the pressure field around the vacuum breaker to determine the flow past the valve. This allows the pressure reduction, due to dynamic effects, to be calculated. A parameter study was undertaken to fix the value of a model parameter by comparisons against experimental data. The adjusted model is shown to provide accurate, but still conservative, estimates of valve impact velocities.

NOMENCLATURE

| | |
|---|---|
| $a$ | chamber radius |
| $A$ | disk area |
| $c$ | speed of sound |
| $f$ | model parameter adjusting strength of Bernoulli torque term |
| $H(\Lambda)$ | height of gap around valve disk |
| $I$ | angular moment of inertia of valve disk |
| $J_n$ | Bessel function of order $n$ |
| $L_D$ | disk pressure moment arm |
| $L_G$ | system gravitational moment arm |
| $mg$ | system weight |
| $p(t)$ | pressure field around valve disk |
| $P(\omega)$ | frequency components (Fourier transform) of $p$ |
| $\hat{P}_{nm}$ | coefficient of nmth spatial harmonic of $P$ |
| $\hat{P}_{00}$ , $\tilde{P}_{00}$ | coefficients of left and right travelling one-dimensional pressure waves respectively |
| $q_{\pm}$ | fluid speed on upstream and downstream sides of valve disk |
| $Q(\theta,t)$ | flow past valve (fluid volume per unit time per unit distance in $\theta$ direction) |
| $(r,\theta,z)$ | right-handed cylindrical coordinate system based at center of closed valve disk |
| $t$ | time |
| $w$ | axial fluid velocity |
| $w_f$ | axial fluid velocity due to flow around the valve disk |
| $x$ | pressure reduction factor to account for upstream dynamic pressure |
| $\beta$ | valve coefficient of restitution |
| $\beta_{nm}$ | value of the argument at the $m$th positive zero of $J_n'$ |
| $\Delta p(t)$ | pressure difference across the valve |

| | |
|---|---|
| $\Lambda$ | valve disk opening angle measured from the closed position |
| $\Lambda_{max}$ | maximum opening angle measured from the closed position |
| $\Lambda_G$ | angle between valve center of mass and vertical with valve in the closed position |
| $\rho$ | fluid density |
| $\sigma_{\pm}$ | orifice coefficients for positive and negative flow |
| $\tau_B$ | Bernoulli torque reduction term |
| $\tau_H$ | total hydrodynamic torque |
| $\omega$ | circular or angular frequency of pressure signal components |

# 1. INTRODUCTION

During the Mark I Full Scale Test Facility (FSTF) containment loads program, a GPE wetwell to drywell vacuum breaker was observed to cycle.[1] In order to assess the structural adequacy of wetwell to drywell vacuum breakers under these cycling conditions, it is necessary to determine the cycling velocities of the valve disk, particularly when and if the valve disk strikes the full open stop or seat. These impact velocities are then either used by a structural analyst to assess the resulting stresses or may be used to define a test program from which the stresses may be measured directly.

In an earlier study, the dynamics of a wetwell to drywell vacuum breaker was simulated by assuming that the hydrodynamic torque $\tau_H$ about the valve shaft which results as a consequence of a differential pressure $\Delta p$ across the valve disk was given by

$$\tau_H = L_D A \Delta p \cos\left(\frac{\pi}{2}\frac{\Lambda}{\Lambda_{max}}\right) \tag{1.1}$$

where $L_D$ is the distance from the shaft to the center of the valve disk of area $A$ (see Fig. 1). The cosine factor was introduced as an approximate reduction of the hydrodynamic torque with valve opening angle $\Lambda$. Assuming that $\Delta p(t)$ is prescribed say from measured test data, the valve motion is estimated by integrating

$$I \frac{d^2\Lambda}{dt^2} + L_G \, mg \sin(\Lambda + \Lambda_G) = \tau_H \tag{1.2}$$

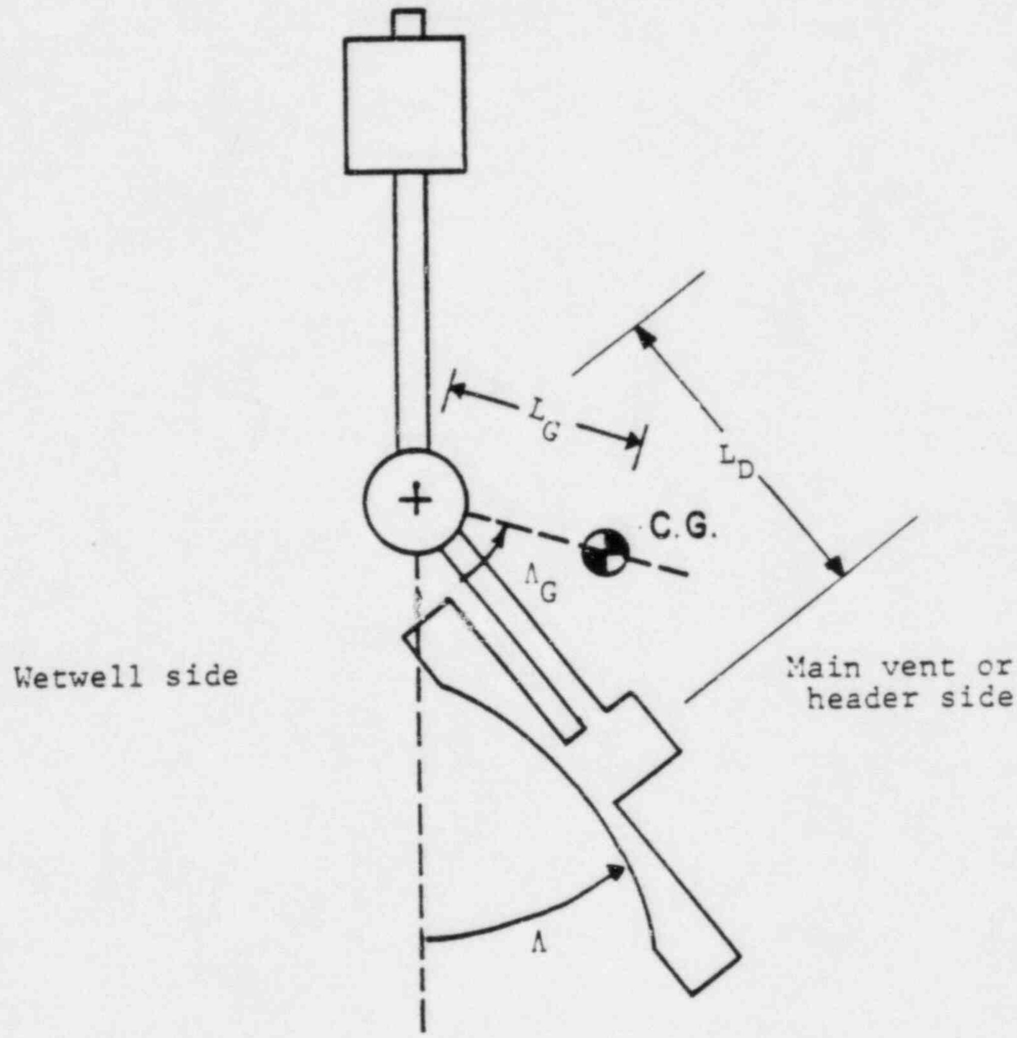


Figure 1. Schematic of a vacuum breaker valve.

subject to the conditions that at

$$\Lambda = 0 \quad \text{or} \quad \Lambda = \Lambda_{max}\,, \quad \left.\frac{d\Lambda}{dt}\right|_{t_+} = -\beta \left.\frac{d\Lambda}{dt}\right|_{t_-} \tag{1.3}$$

The constant $\beta$ is a coefficient of restitution and fixes the fraction of kinetic energy lost during impact.

During FSTF run S-DA, a GPE vacuum breaker mounted on the ring header was instrumented such that valve displacement and pressure differential across the valve disk were recorded as a function of time. This test (S-DA) permitted a comparison to be made between predictions of valve displacement/velocity and actual measured displacement/velocity. Predictions were made by specifying the measured differential pressure across the valve (shown in Figure 2) and integrating in Eq. (1.2) with the valve geometric and inertial parameters specified in Table 1. The result of this comparison is summarized in Figure 3 where measured closing impact velocities are compared to predicted impact velocities. (No impacts of the valve displacement with the full open stop were observed or predicted.)

The scatter plots in Figure 3 and later figures were generated by considering the 28 chugs in run S-DA, during which all significant valve actuation took place. These chugs were distributed through 50 seconds of the S-DA run. During many of these chugs, there were a number of seat impacts, because the valve bounced. In such cases, the maximum impact velocity was used. Thus, each symbol on the scatter plot graphs the maximum predicted impact velocity during a particular chug against the maximum experimental impact velocity for the same chug. The particular geometric symbol used for a given point shows which 10 second time

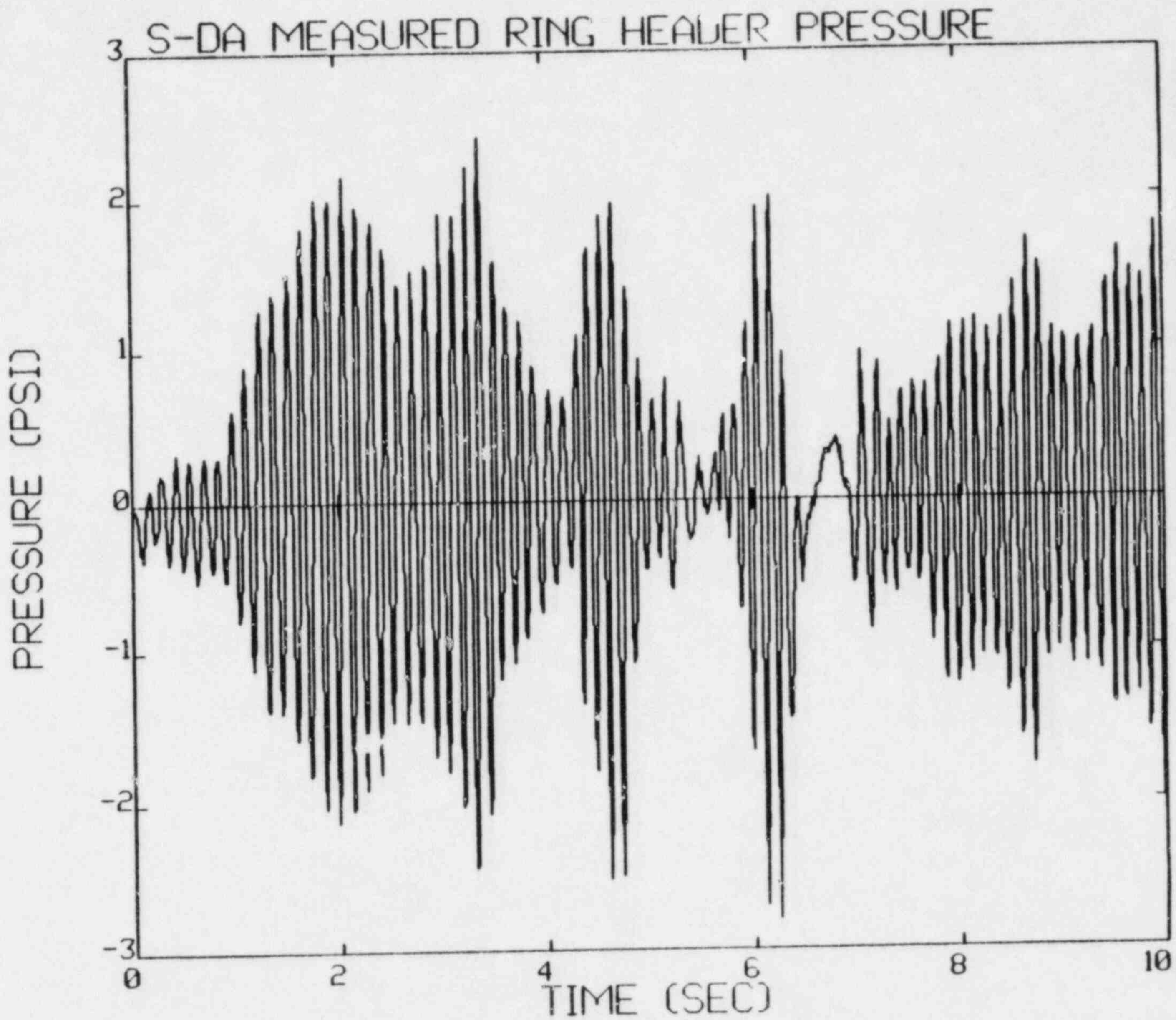


Figure 2. Measured ring header pressure during run S-DA, with linear trend removed. Submergence head removed. a) First 10 seconds.

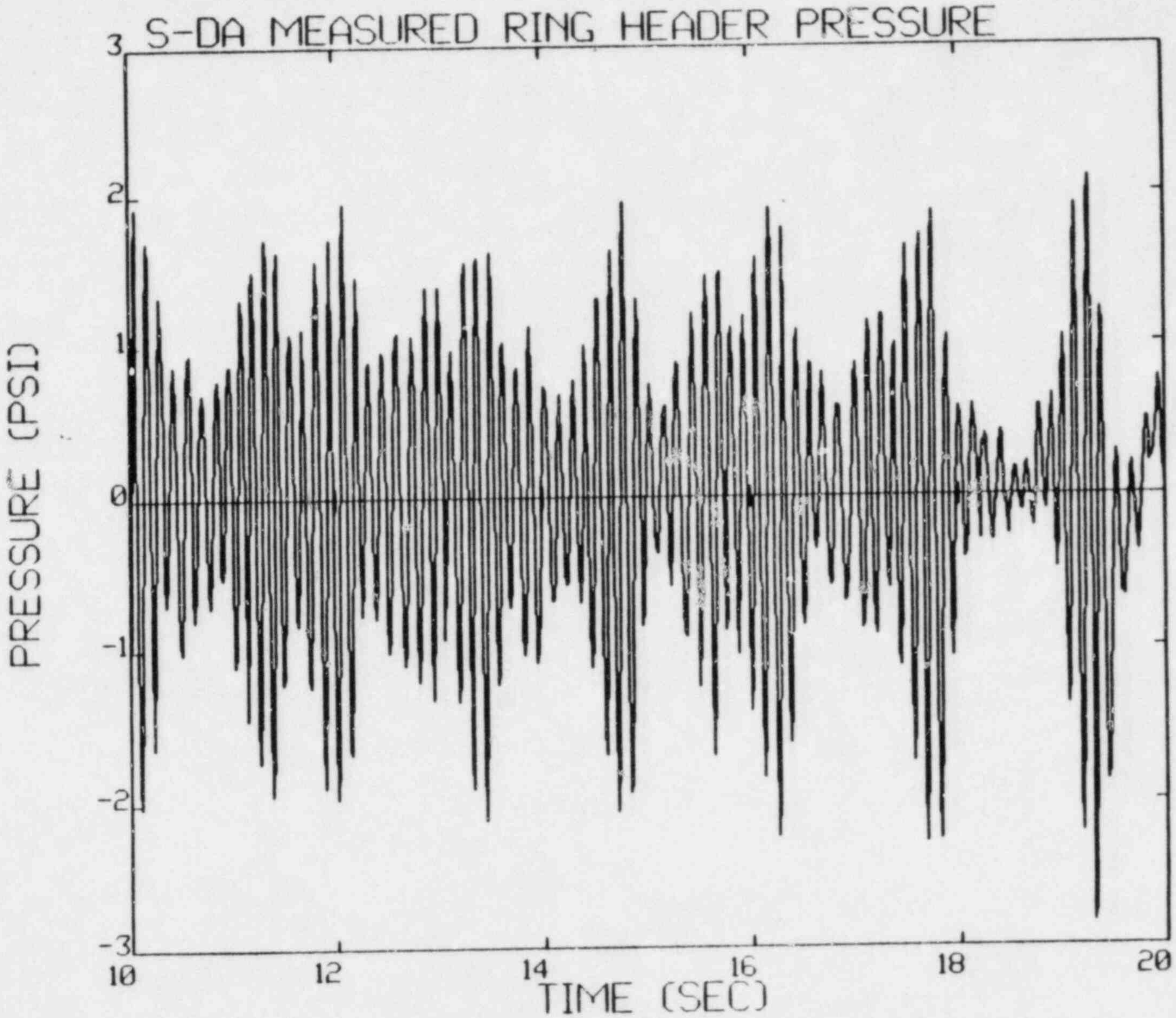


Figure 2b. Second 10 seconds.

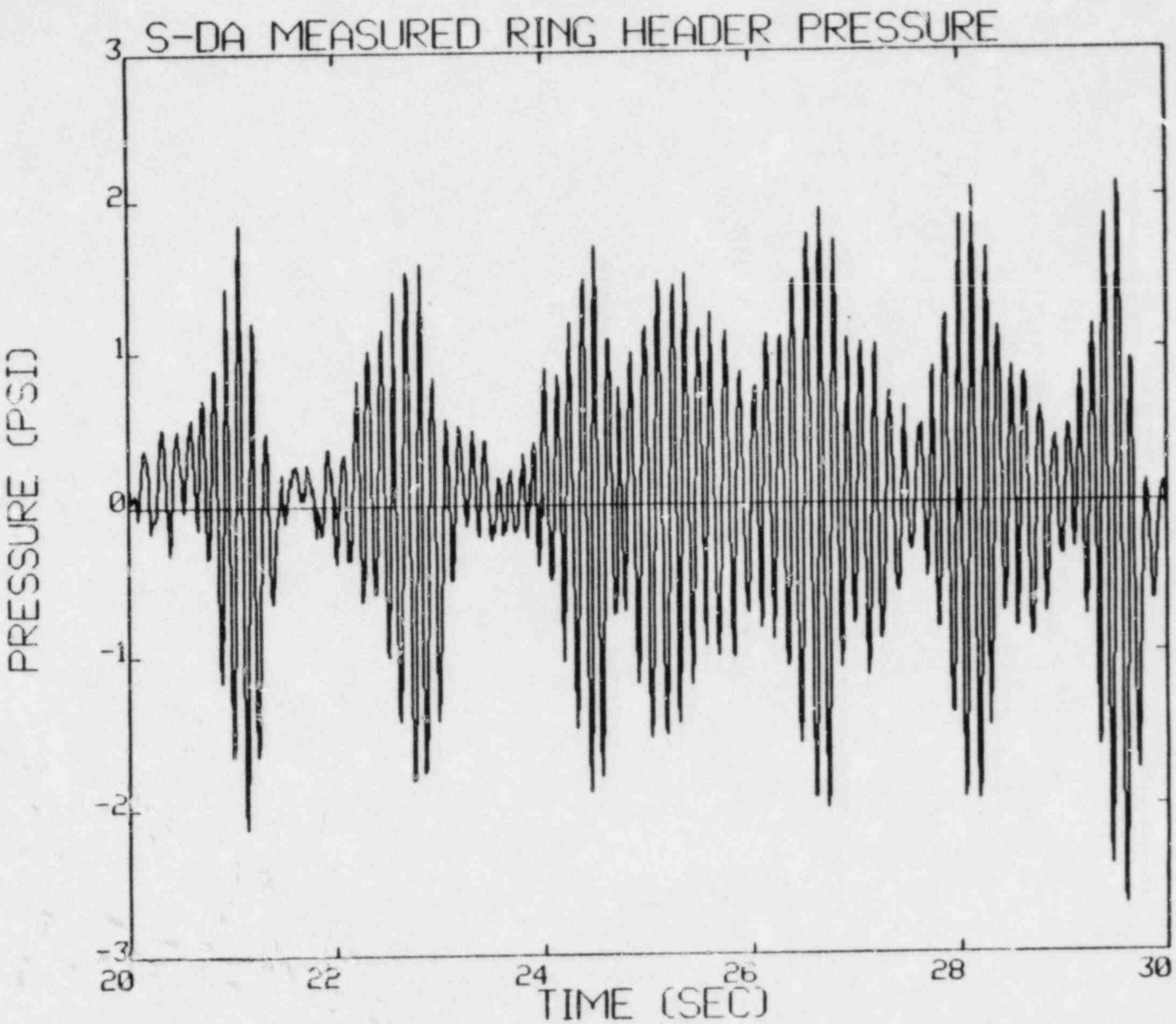


Figure 2c. Third 10 seconds.

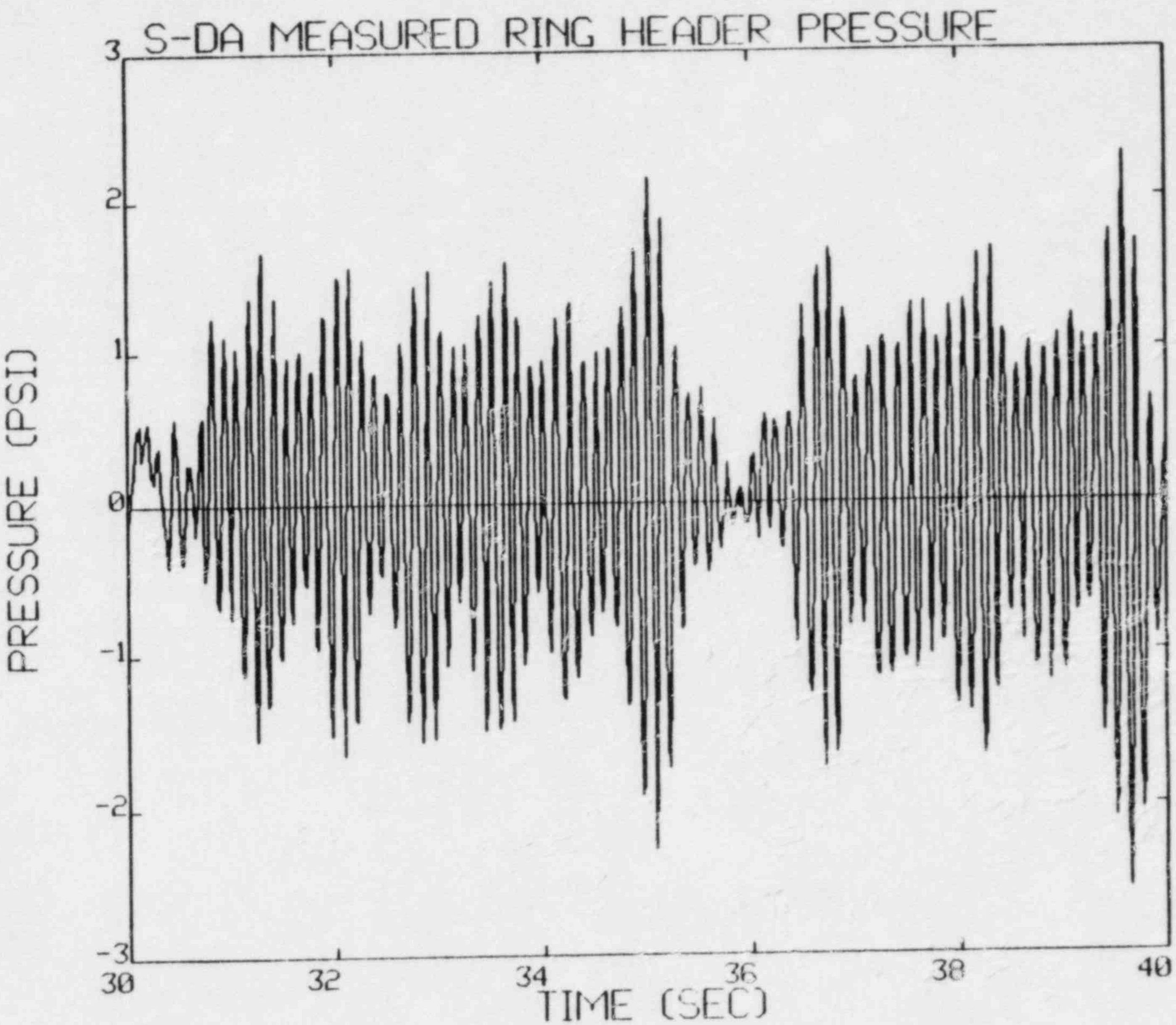


Figure 2d. Fourth 10 seconds.

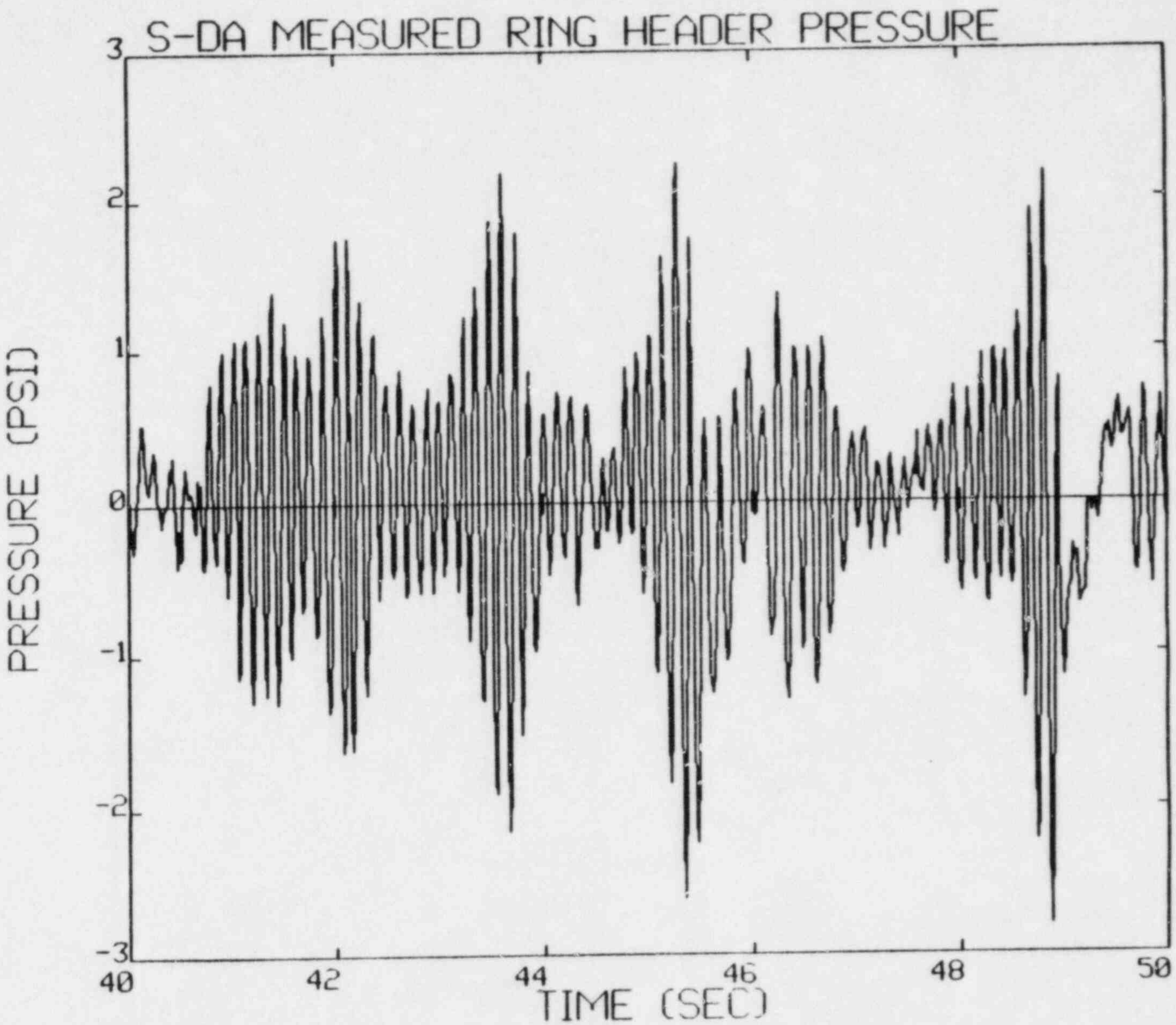


Figure 2e.  Fifth 10 seconds.

TABLE 1

GPE 18" Internal Valve Characteristics

| | GPE 18" INTERNAL |
|---|---|
| $I$ , system moment of inertia ($lb\text{-}in\text{-}s^2$) | 20.38 |
| $L_G$ , system moment arm (in) | 10.71 |
| $L_D$ , disk pressure moment arm (in) | 11.47 |
| $m$ , system mass (lb) | 50.9 |
| $A$ , disk area ($in^2$) | 375.82 |
| $\Lambda_G$ , rest angle (rad) | 0.0 |
| $\Lambda_{max}$ , maximum opening angle (rad) | 1.32 |
| $\beta$ , coefficient of restitution (seat and body) | 0.6 |

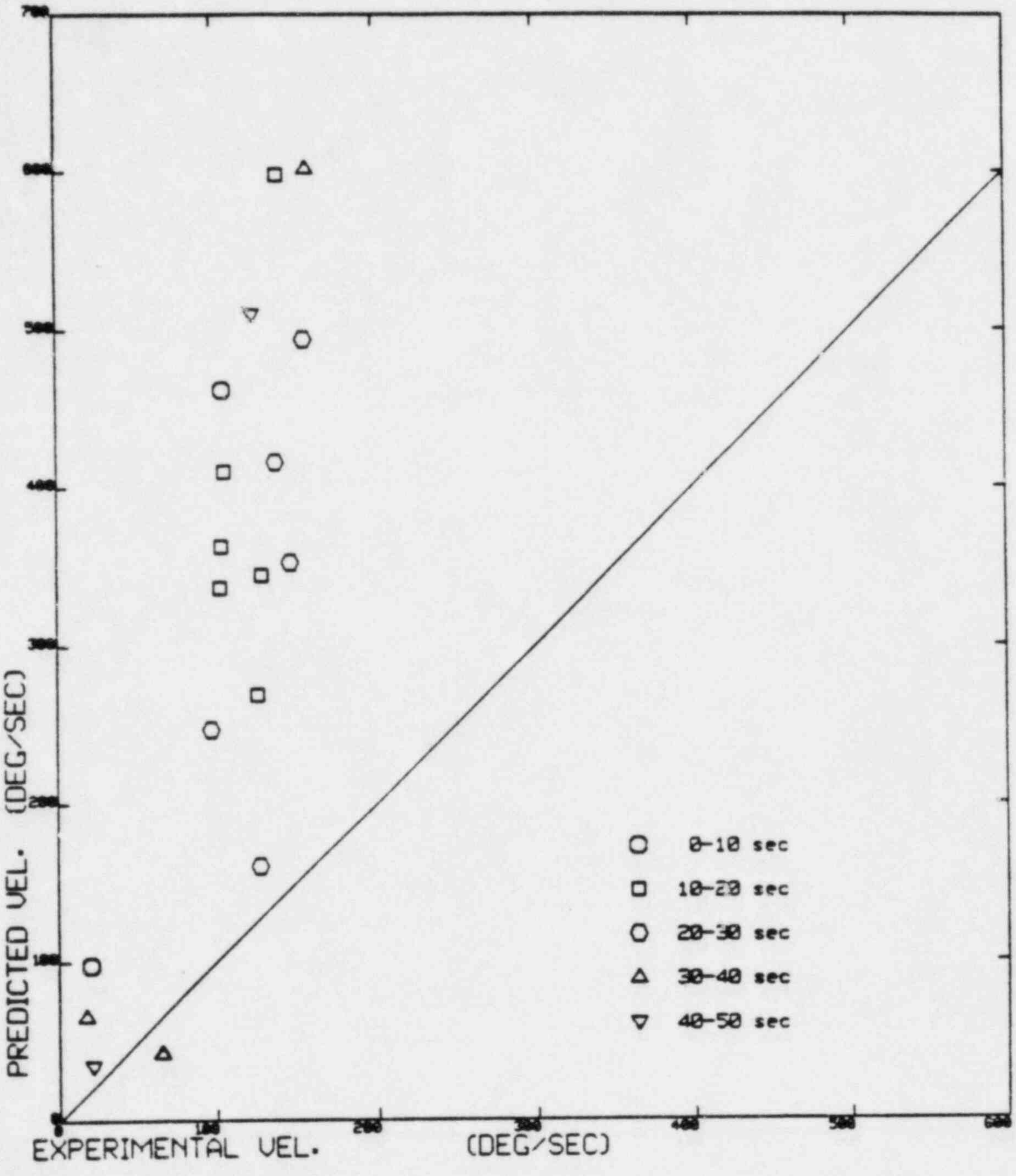


Figure 3. Comparison of experimental and predicted closing disk impact velocities for run S-DA. Hydrodynamic torque computed from Eq. (1.1)

period of run S-DA the corresponding impact was within, as indicated in the plot label. (No correlation between impact velocities and run time was observed.)

It should be noted that the experimental velocities used were derived from measured digitized time history of valve position by a two point method

$$\dot{\Lambda}_{n+\frac{1}{2}} = \frac{(\Lambda_n - \Lambda_{n+1})}{\Delta t} \tag{1.4}$$

which provides a considerably more conservative and probably also more accurate estimate of impact velocities than a three-point parabolic fit method would.

As can be seen, the predicted impact velocities were greater than the experimental impact velocities by an average factor of more than 2½. For this reason, an analytic effort described below was initiated to develop a valve dynamic model which would more realistically estimate actuation velocities of vacuum breaker disks under transient loading conditions.

## 2. VALVE MODEL - ANALYSIS

The very conservative prediction of valve actuation velocities results from the fact that flow across the valve disk reduces the hydrodynamic torque generated on the disk to less than that estimated from Eq. (1.1). In order to more appropriately account for this reduction of hydrodynamic torque resulting from flow through the valve it is proposed to estimate the actual pressure distribution on the valve disk by analytically computing the fluid velocity distribution about the valve disk and then estimating the corresponding pressure and integrating this pressure over the valve area to compute hydrodynamic torque. The analysis will be to compute the hydrodynamic torque $\tau_H$ such that

$$\tau_H = L_D A \Delta p(t) - f\tau_B \tag{2.1}$$

The quantity $L_D A \Delta p(t)$ is the estimate of hydrodynamic torque which results when no credit is taken for the reduction of static pressure across the valve disk as a consequence of flow. The quantity $\tau_B$ is the torque reduction which results as a consequence of flow through the valve and will be estimated from an analysis which assumes that the valve disk undergoes small displacements. For this reason, a factor $f$ is introduced which will be fixed by comparison of the model predictions against data.

In the function $\tau_B$ the subscript B denotes Bernoulli since the reduction of torque results primarily from a reduction of the static pressure by dynamic pressure. This result is a consequence of the fact that although the valve disk may be in motion, the fluid flow field is approximately quasi-steady. It may be shown that the reduced frequency for the valve motion

considered here is indeed small and hence fluid acceleration effects may be neglected. Therefore, the Bernoulli torque is given by

$$\tau_B = \int_{r<a} \tfrac{1}{2}\rho(q_+^2 - q_-^2)(a - r\cos\theta)\, r\,dr\,d\theta \qquad (2.2)$$

where $q_+^2$ and $q_-^2$ are the fluid velocity squared on the upstream and downstream side of the valve disk (as shown in Figure 4) respectively.

The task now is to estimate $q_\pm^2$. This is accomplished by noting that the fluid is nearly incompressible and hence the pressure field satisfies $\nabla^2 p = 0$. General solutions to this equation are found upstream and downstream of the valve disk with the boundary condition at the valve disk that the fluid velocity $w$ along the valve axis is

$$w = \frac{d\Lambda}{dt}(a - r\cos\theta) + w_f \qquad (2.3)$$

where $w_f$ is the flow velocity through the valve shown in Figure 4. The flow velocity through the valve is estimated from

$$Q(\theta,t) = \frac{\pm\, \sigma_\pm H(\Lambda)\left(\frac{1-\cos\theta}{2}\right)\sqrt{\frac{2}{\rho}|\Delta p|}}{x} \qquad (2.4)$$

where $Q$ is the volumetric leakage flow per unit circumferential length around the valve body and $H(\Lambda)\left(\frac{1-\cos\theta}{2}\right)$ is the height of the annular flow area with the valve open. The factor $\sigma$ is an orifice coefficient and is left as model parameter. $\sigma$ has been taken to be 1.0 for positive flow and 0.6 for negative flow. The $x$ factor is used to account for the reduction of upstream pressure due to nonnegligible upstream flow velocity at large

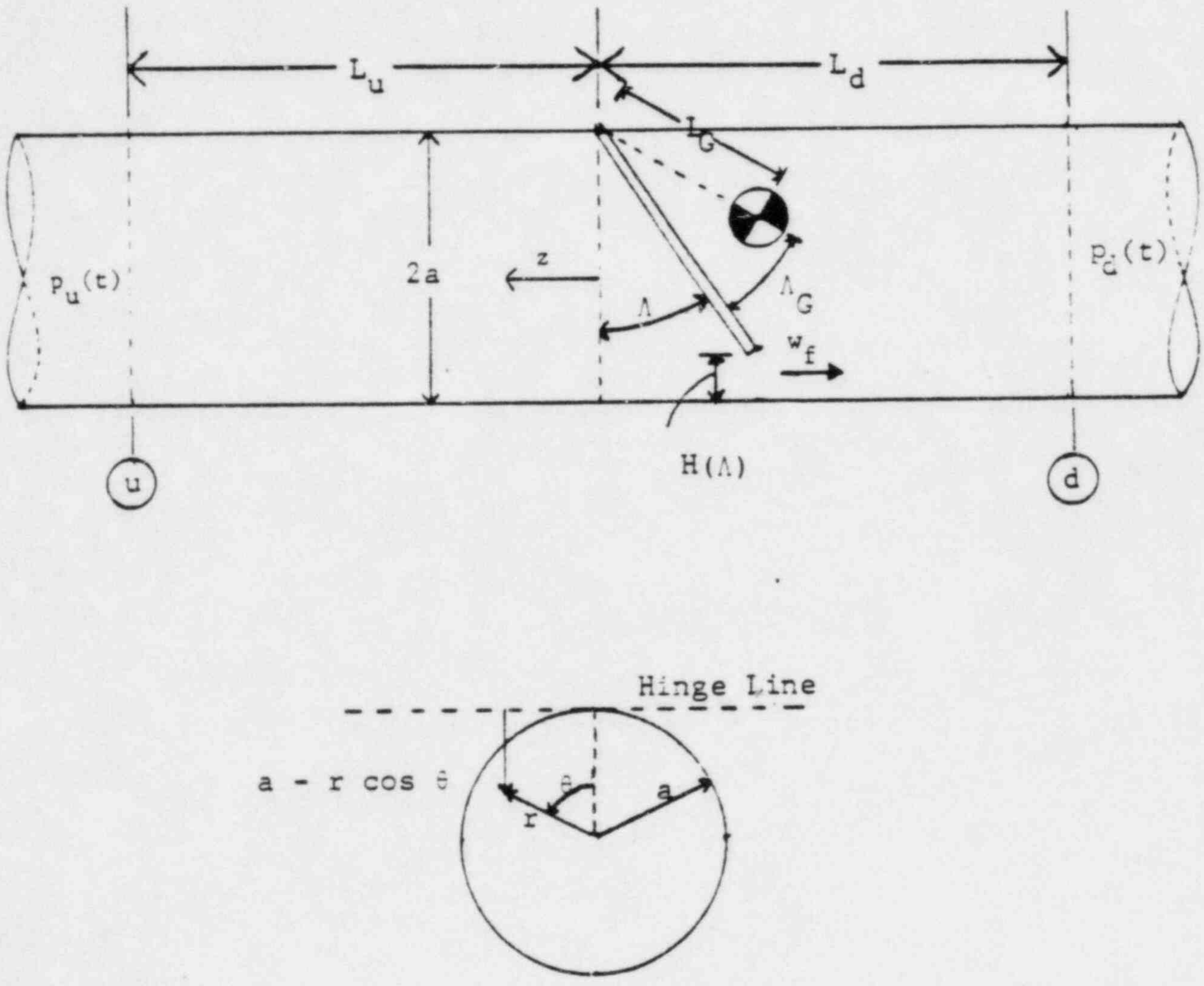


Figure 4. Single Valve Model Geometry.

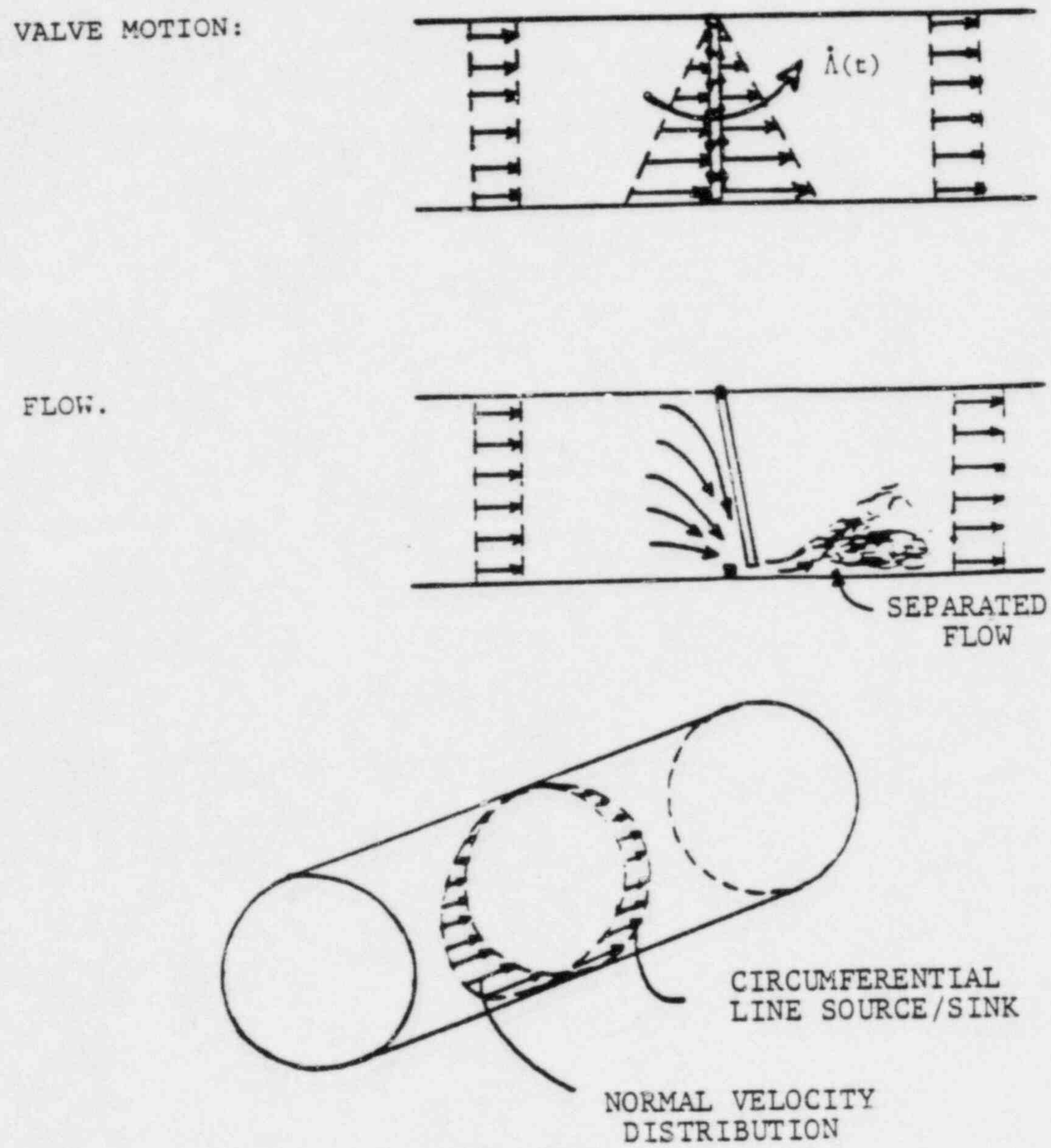


Figure 5. Schematic of fluid flow field in the vicinity of the valve disk.

valve opening angles. This factor may be shown to be equal to

$$x = \sqrt{1 - \left( \frac{H}{a} - \frac{3}{8}\left(\frac{H}{a}\right)^2 \right)^2} \tag{2.5}$$

The volumetric flow through the valve $Q$ is related to $w_f$ by distributing the flow as an annular source as sketched in Figure 5. The flow field at the valve disk is related to the pressure field by

$$\frac{\partial w}{\partial t} = - \frac{1}{\rho} \frac{\partial p}{\partial z} \tag{2.6}$$

where the general solution for pressure is

$$P(\omega) = \left( \hat{P}_{00} e^{i\omega z/c} + \tilde{P}_{00} e^{-i\omega z/c} + \sum_{n=0}^{\infty} \sum_{m=1}^{\infty} J_n\left(\beta_{nm} \frac{r}{a}\right) \cos n\theta \right.$$

$$\left. \hat{P}_{nm} e^{-\beta_{nm} z/a} \right) e^{i\omega t} \tag{2.7}$$

for one frequency component. With the orifice coefficients fixed the above model has one free modeling constant, $f$ . This constant is determined by comparison against full scale test data.

## 3. VALVE MODEL - VERIFICATION

As discussed in the Introduction, FSTF run S-DA was instrumented to obtain valve displacement data as well as to measure the differential pressure across the valve disk. By driving the valve dynamic model with the measured differential pressure across the valve, predictions of valve displacement versus time are made and compared against measured data. Referring back to Figure 2, the pressure measured in the ring header during FSTF run S-DA is shown over a 50 second interval during which strong pressure oscillations were observed. The mean has been removed from this data. The measured valve displacement over this time interval is shown in Figure 6 where a maximum valve displacement of 18° is observed to occur at time 19.5 seconds.

The valve model impact velocity predictions with $f = 1$ are compared with measured data in Figure 7. As can be seen, the predicted impacts are still very conservative with regard to measured closing impact data. To reduce this conservatism further, a parameter study was undertaken and it was determined that with $f = 2.25$ predicted valve impact velocities would still bound all test impact data with approximately a 12% margin. The predicted valve displacement versus time is shown in Figure 8. These predictions may be compared to the measured displacements shown in Figure 6 from which it will be seen that the comparisons are very favorable. In Figure 9 is shown the predicted and measured closing impact velocities which illustrate that conservatism in the analytic valve dynamic model has been minimized. Lastly, in Table 2 the results of model comparisons with data are summarized. It should be noted that this valve dynamic model with

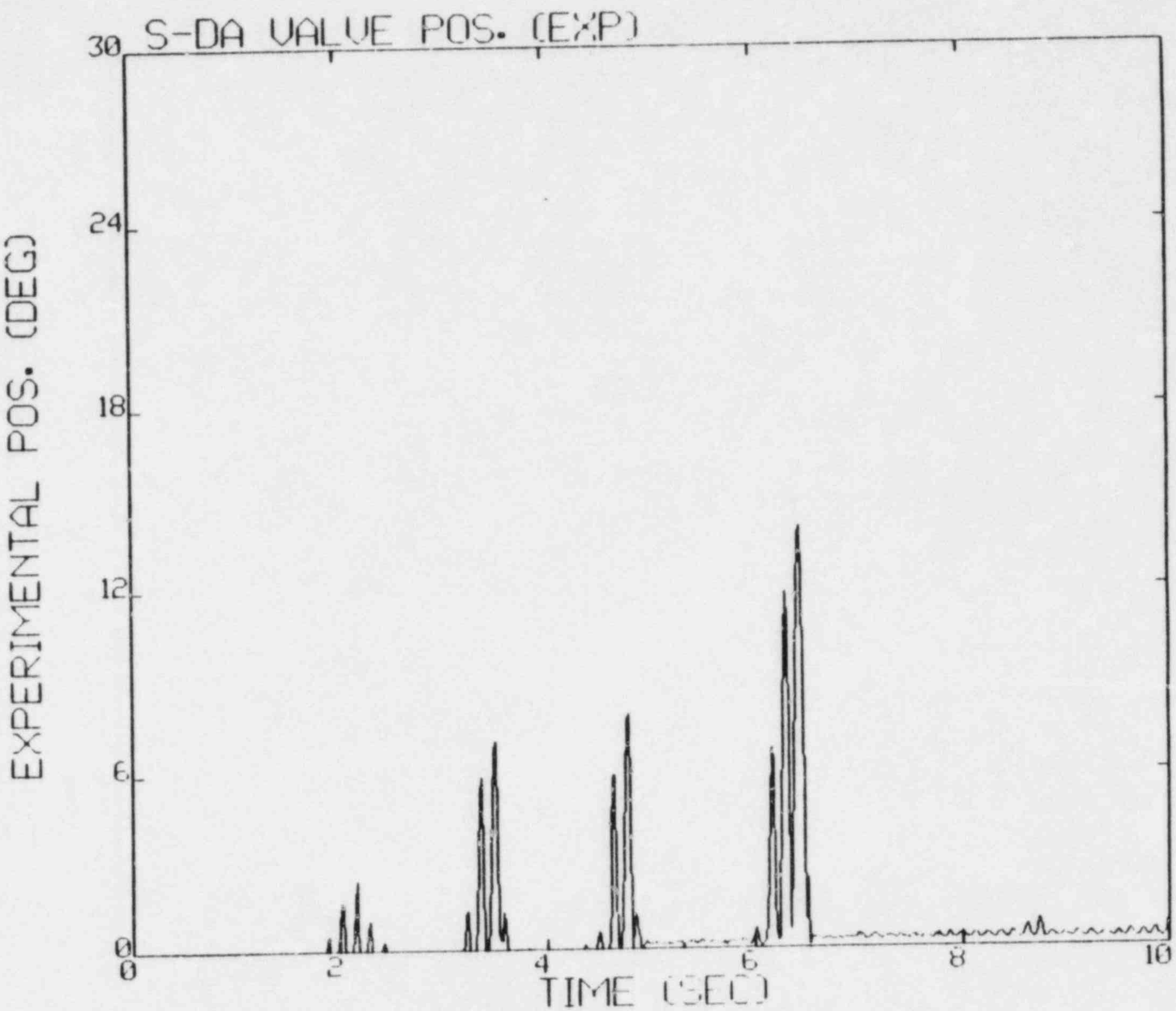


Figure 6. Measured vacuum breaker disk angle during run S-DA.
a) First 10 seconds.

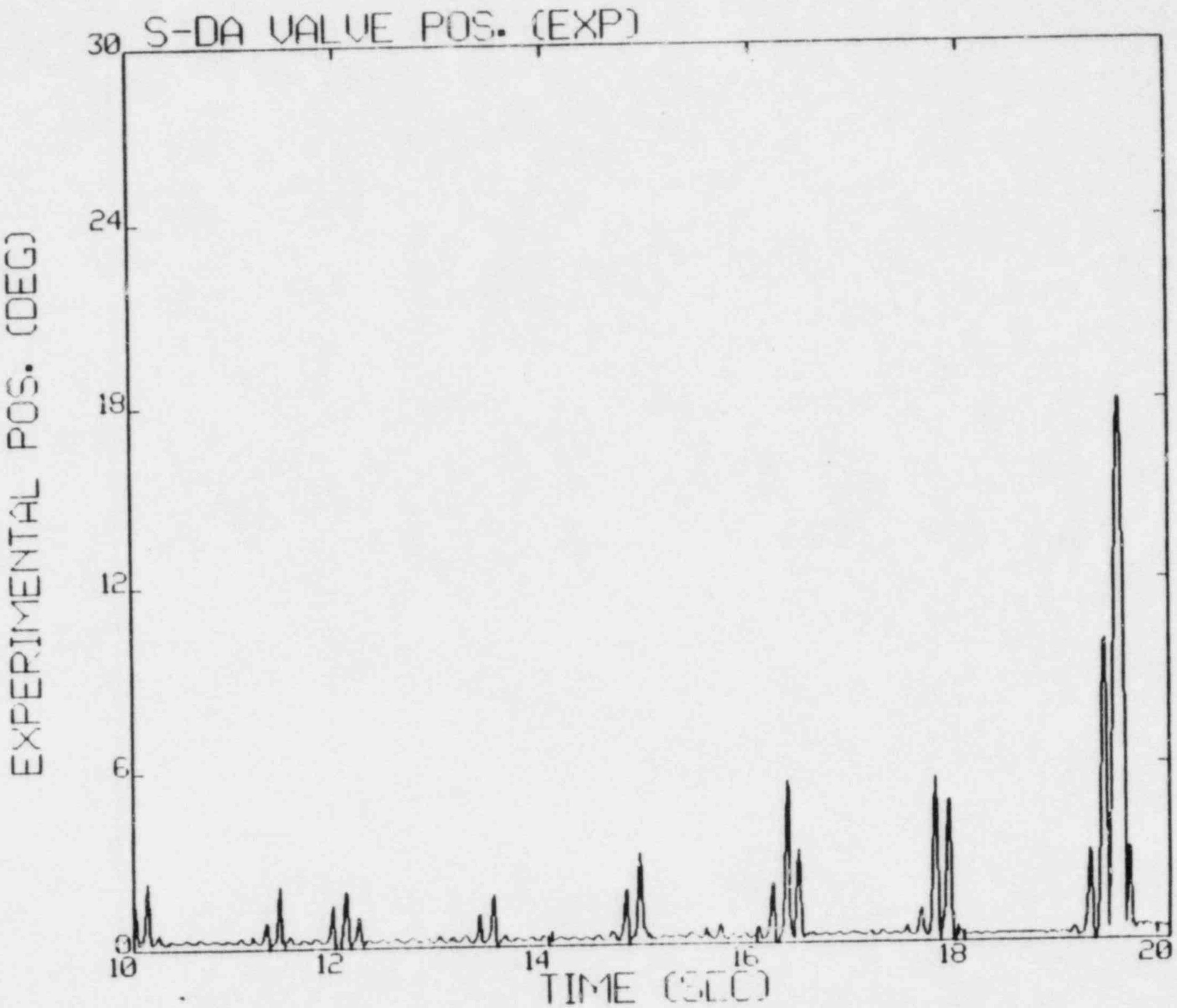


Figure 6b. Second 10 seconds.

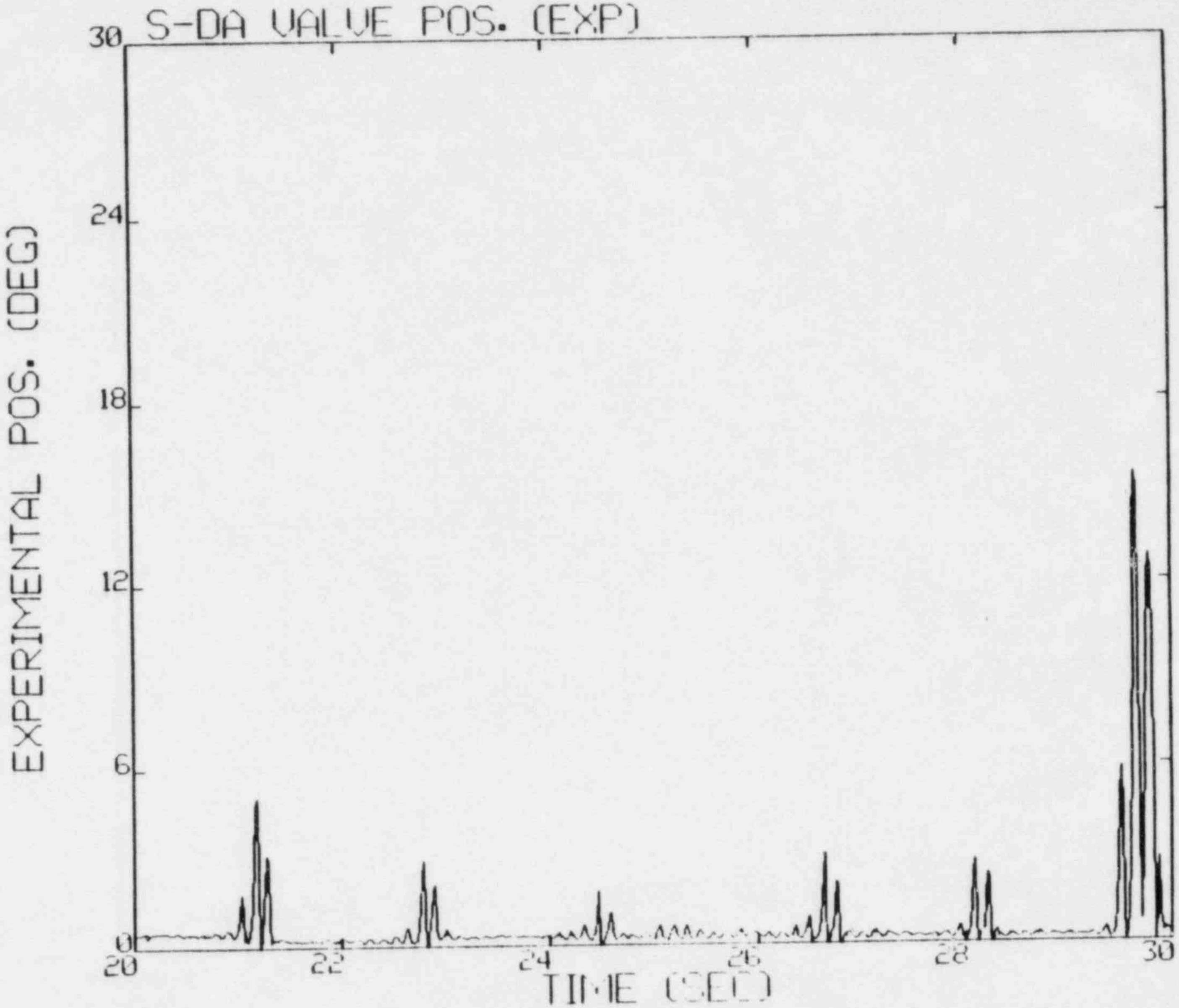


Figure 6c. Third 10 seconds.

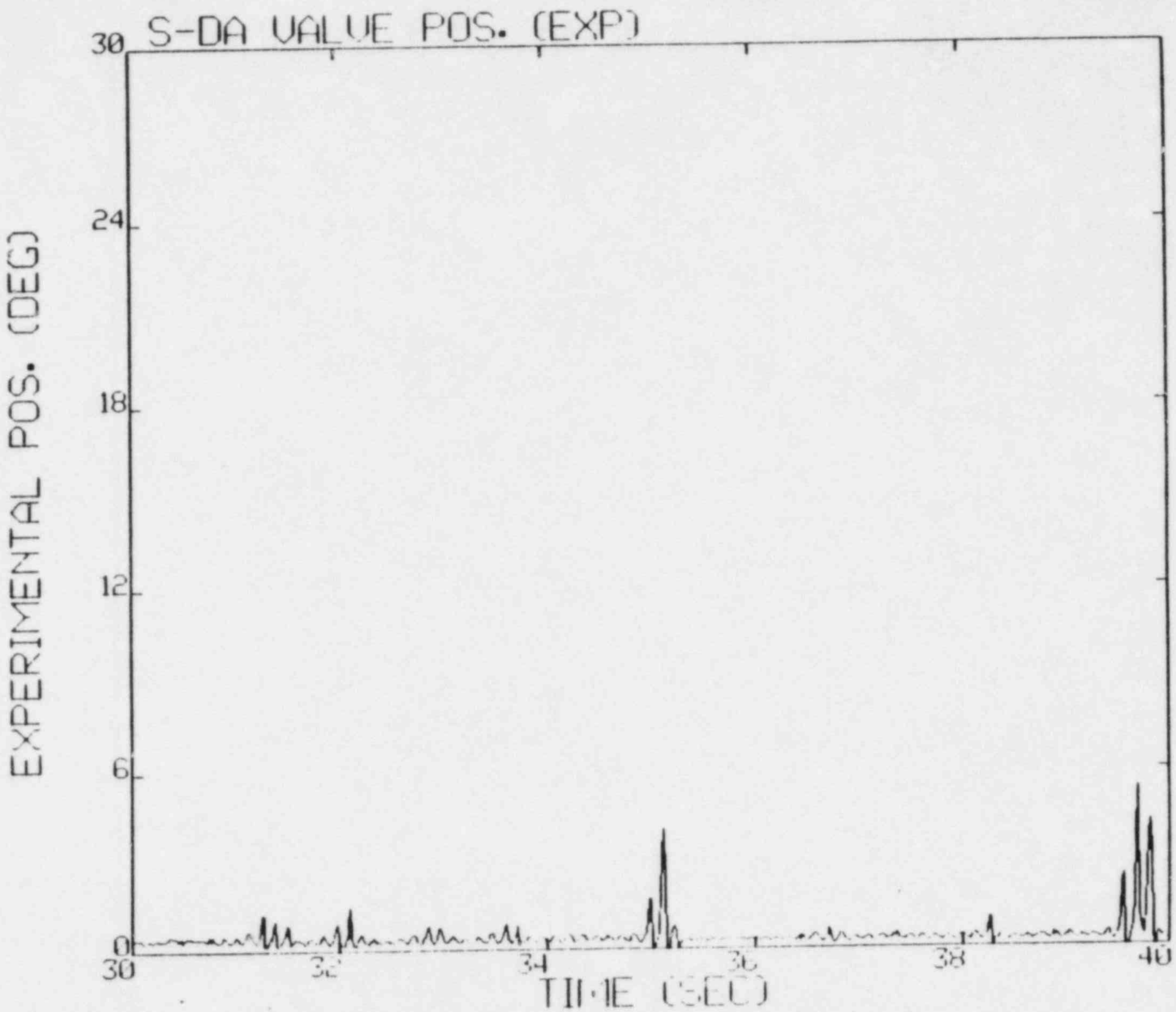


Figure 6d. Fourth 10 seconds.

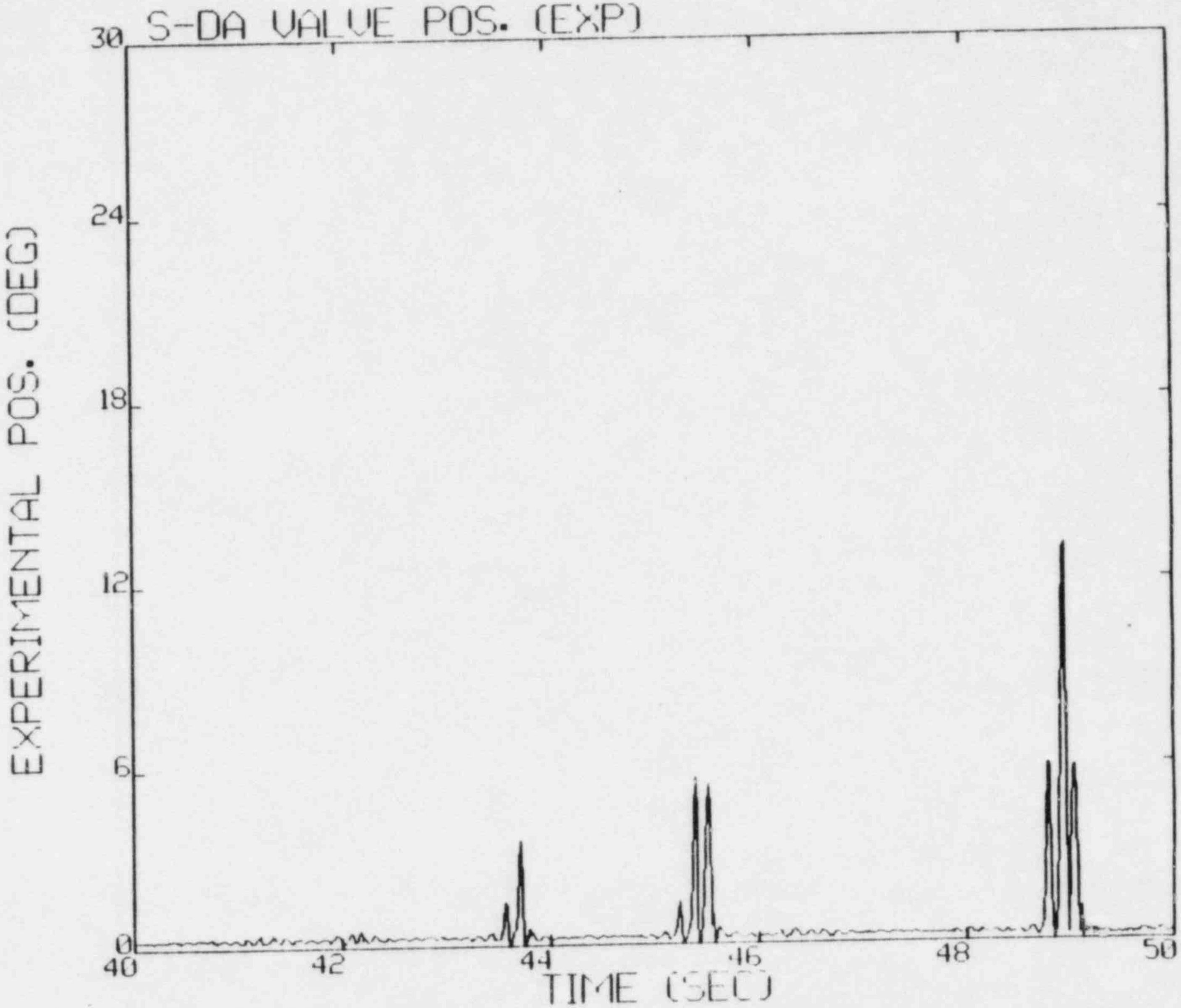


Figure 6e. Fifth 10 seconds.

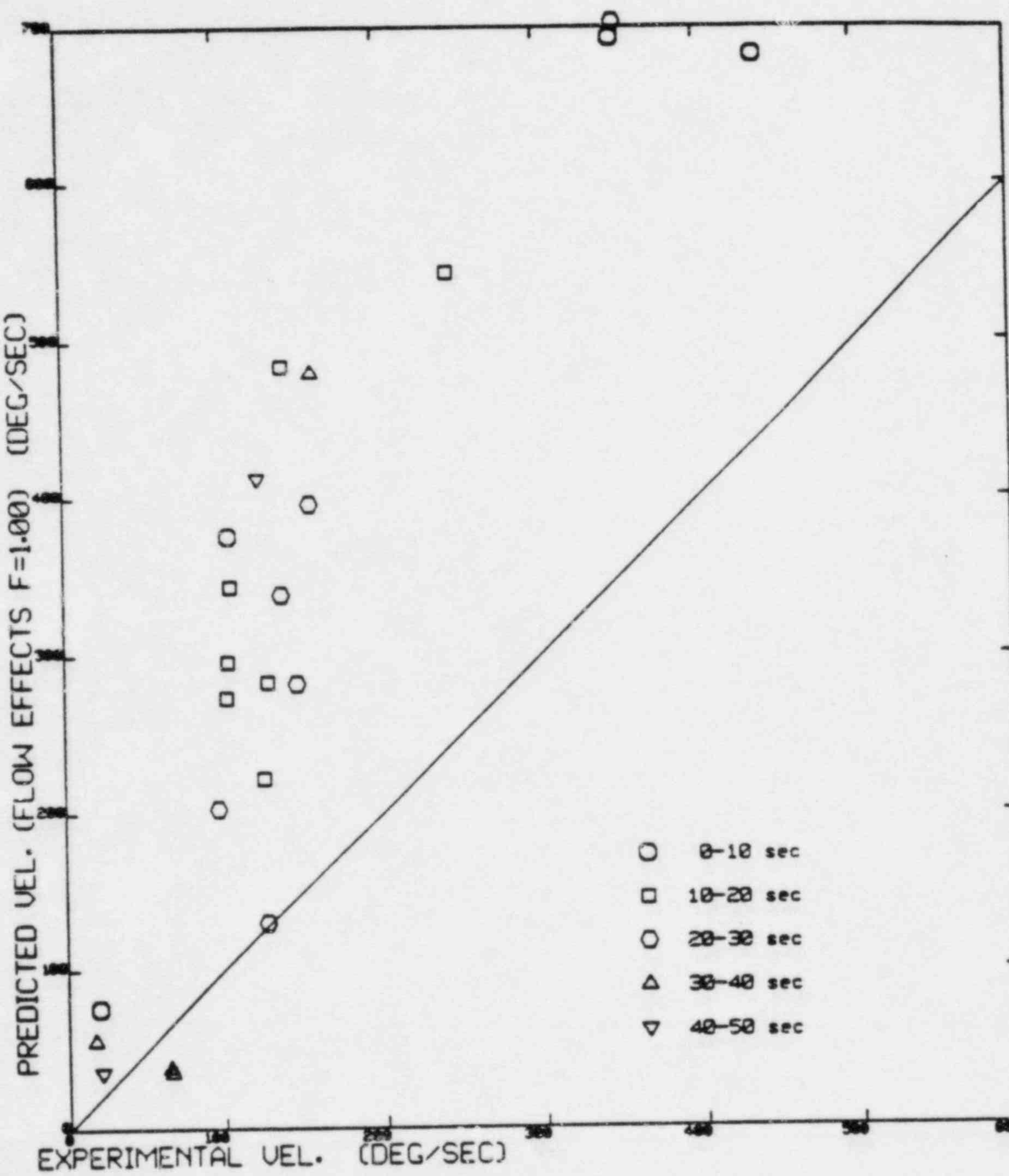


Figure 7. Comparison of experimental and predicted closing impact velocities for run S-DA, f = 1 .

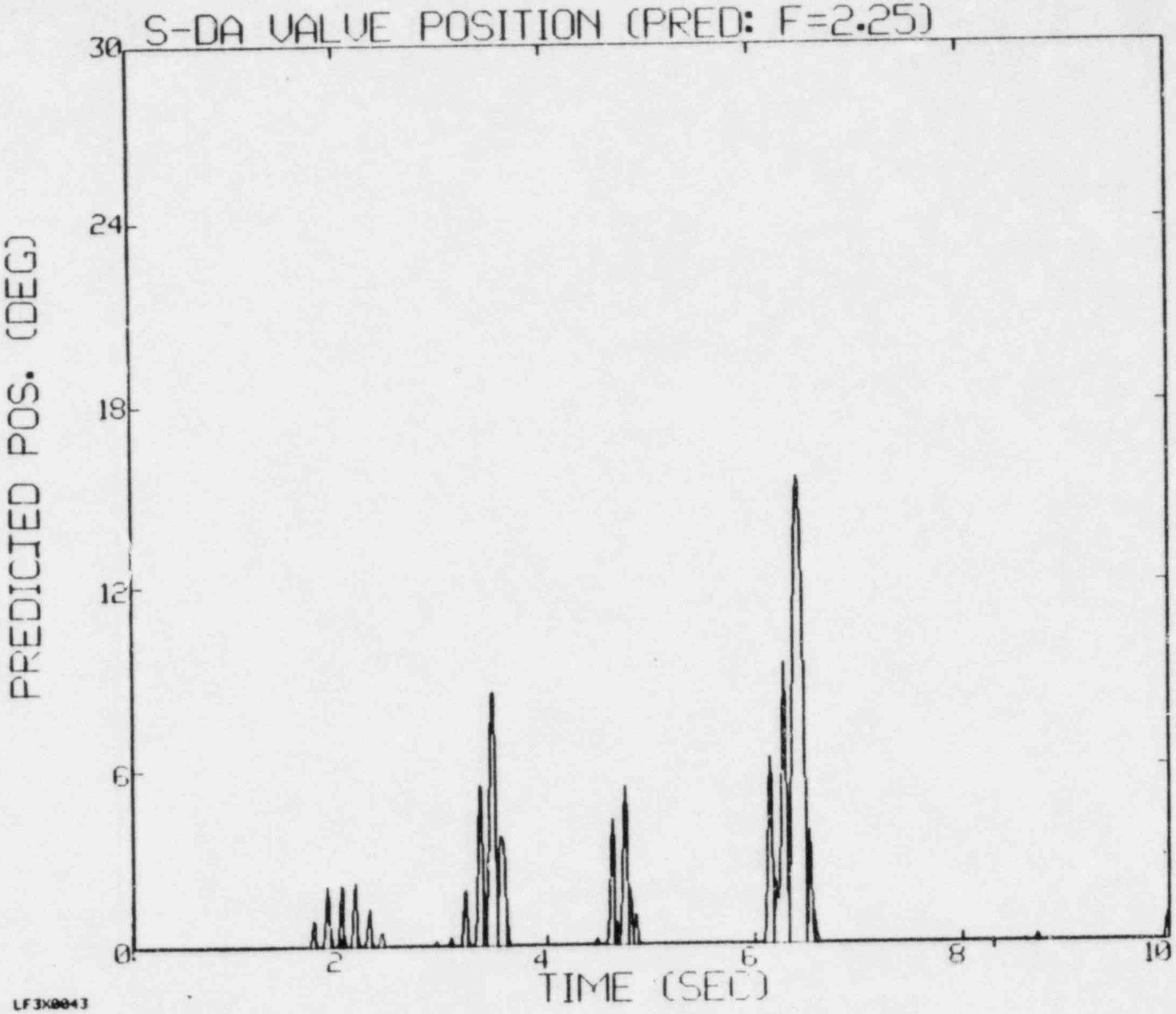


Figure 8. Predicted vacuum breaker disk angle for run S-DA (using model with flow effects f = 2.25). a) First 10 seconds.

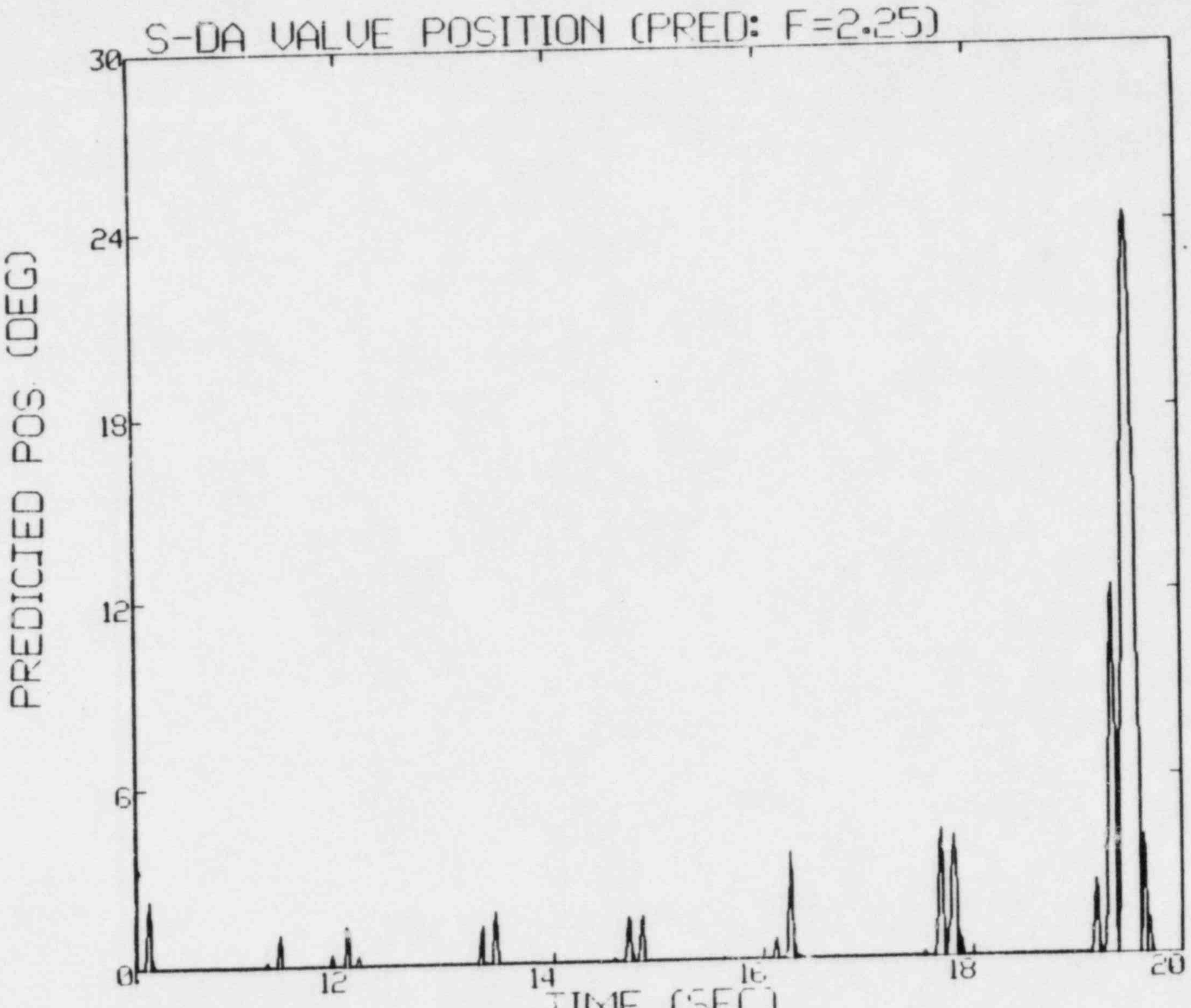

LF3X0043

Figure 8b. Second 10 seconds.

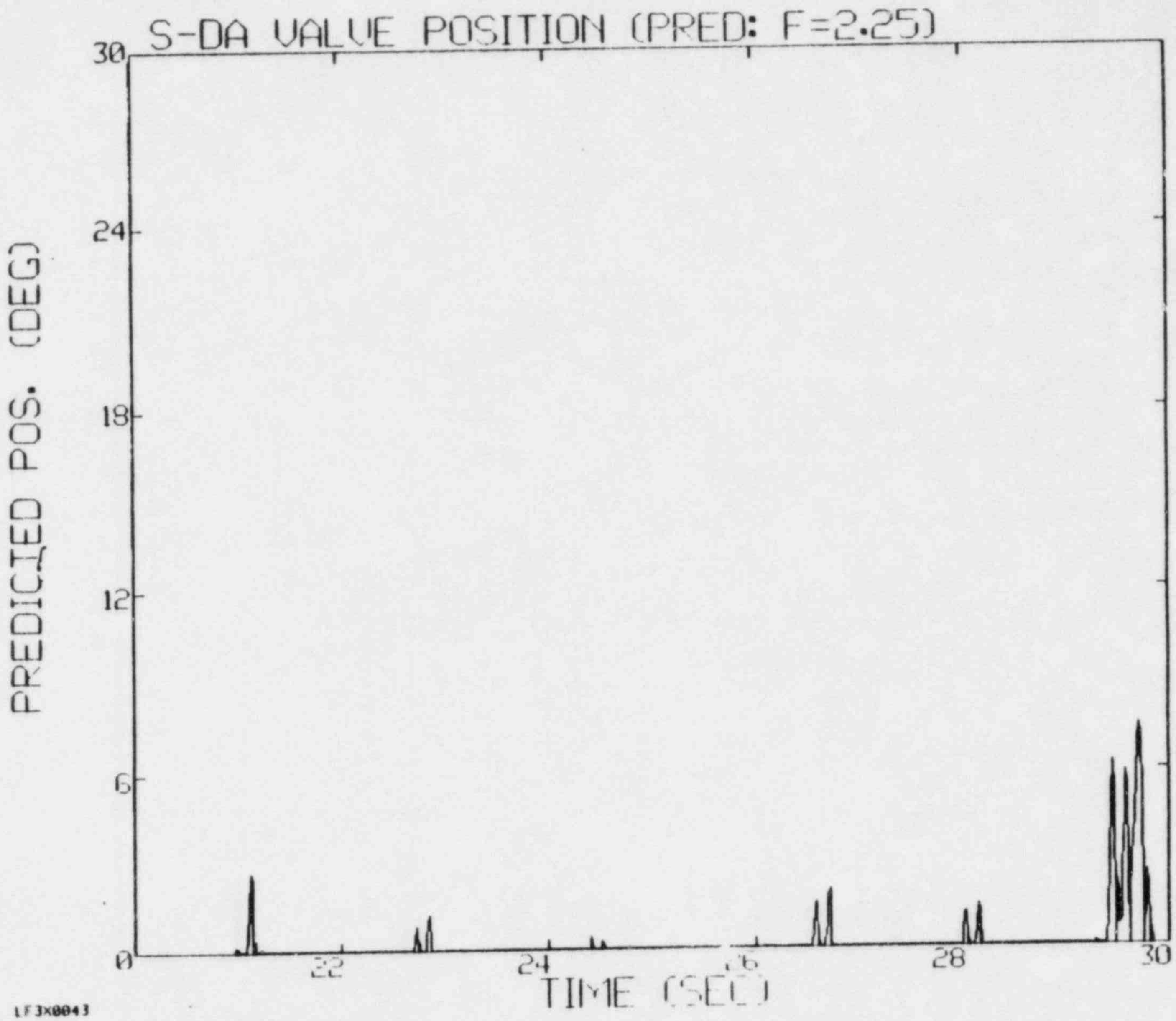


LF3X0043

Figure 8c. Third 10 seconds.

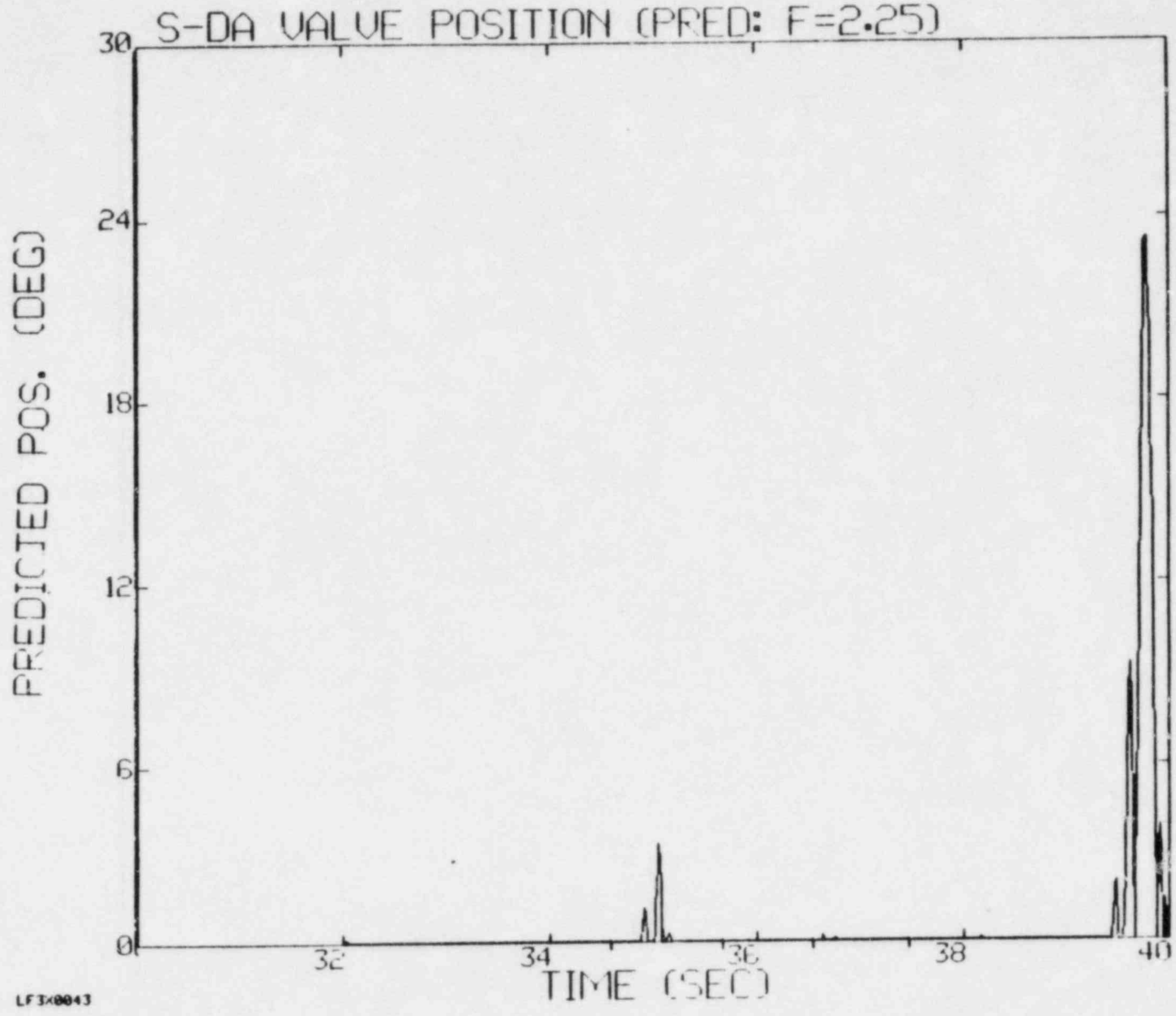


Figure 8d. Fourth 10 seconds.

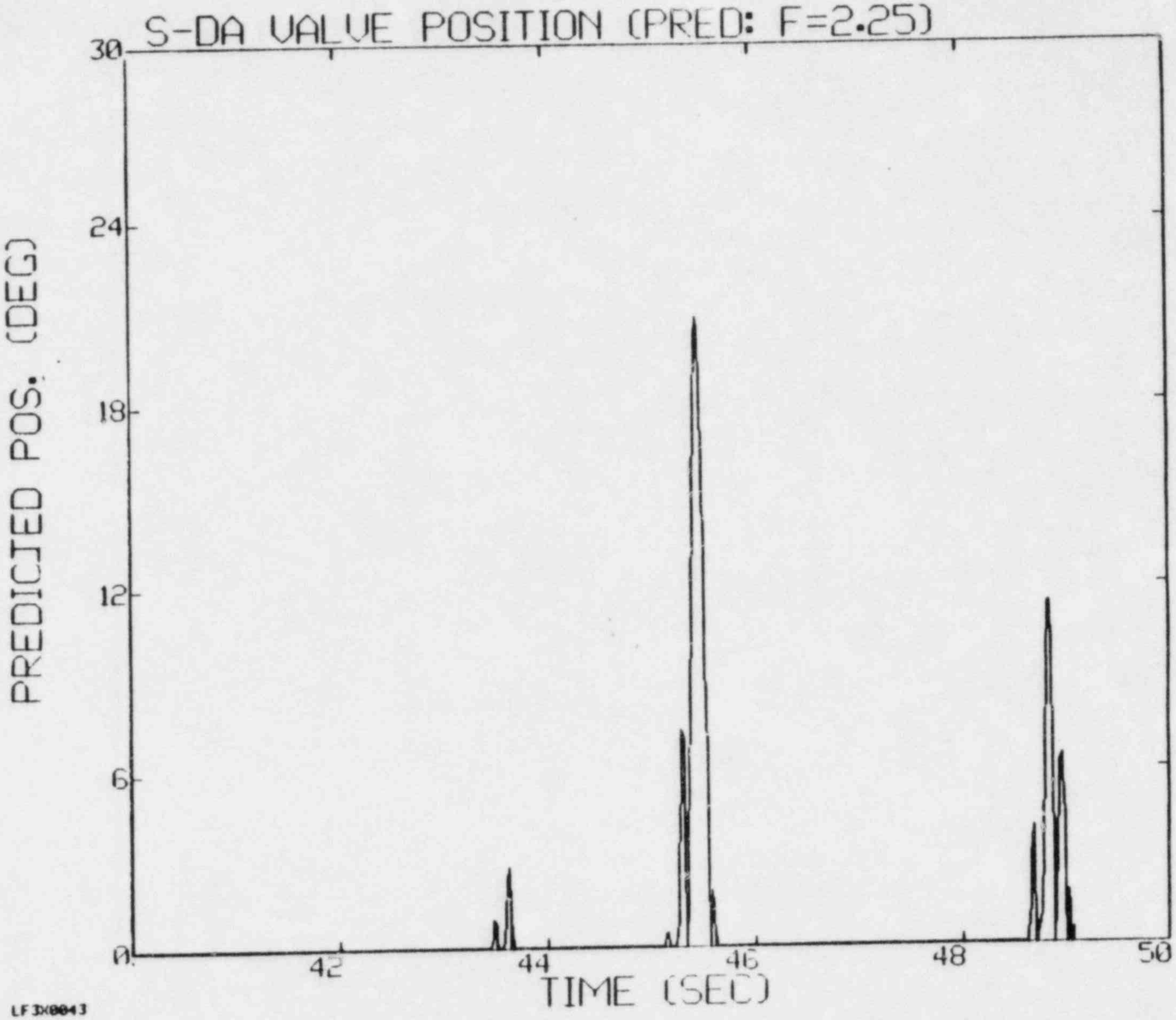


Figure 8e. Fifth 10 seconds.

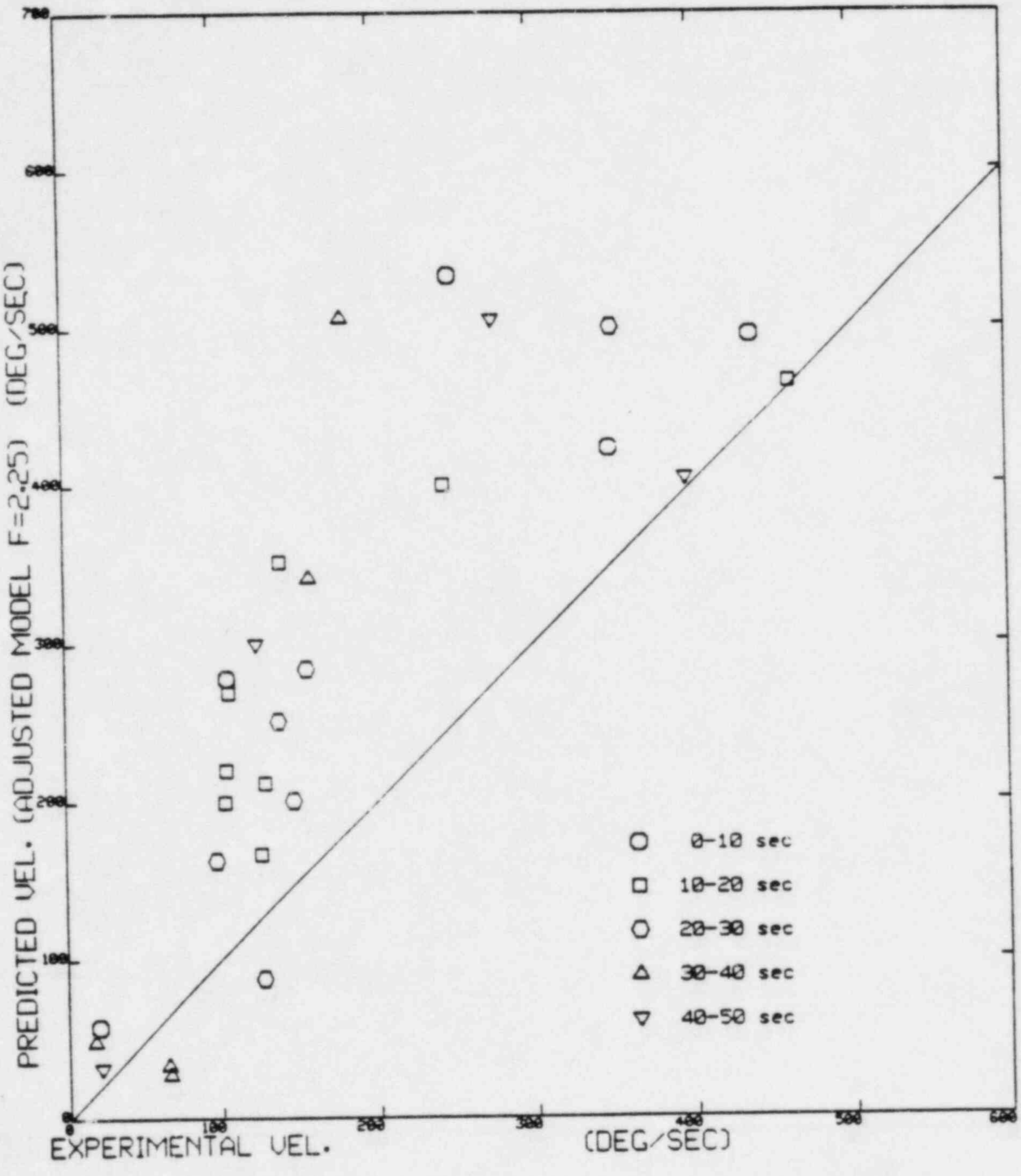


Figure 9. Comparison of experimental and predicted closing impact velocities for run S-DA, f = 2.25, —— adjusted model with minimized conservatism.

TABLE 2

GPE Valve Response to S-DA Measured Pressure Signal

| | Maximum Seat Impact Velocity (rad/sec) | Number of Impacts above -7.5 rad/sec | Maximum Open (rad) |
|---|---|---|---|
| Original Model (f = 1.00) | -14.35 | 25 | 0.73 |
| Adjusted Model (f = 2.25) | -9.31 | 8 | 0.42 |
| GPE Measured Impact Velocities | -8.06 | 2 | 0.34 |

$f = 2.15$ over predicts the maximum observed closing impact velocities by approximately 12%.

It is concluded that the valve dynamic model results in realistic yet conservative predictions of valve actuation velocities and is therefore appropriate for the analysis and/or qualification of Mark I wetwell to drywell vacuum breakers.

## 4. REFERENCES


1. "Mark I Containment Program; Full Scale Test Program; Final Report," NEDE-24539-P, Class III, General Electric Company, April 1979.